REPORT DOCUMENTATION PAGE

Form Approved
OMB No. 0704-0188

1. REPORT DATE *(DD-MM-YYYY)*	2. REPORT TYPE	3. DATES COVERED *(From - To)*
2/28/14	Final Technical Report	9 July 2007-8July 2009

4. TITLE AND SUBTITLE
High Speed Laser with > 100 GHz Resonance Frequency

5a. CONTRACT NUMBER

5b. GRANT NUMBER
W911NF-07-01-0468

5c. PROGRAM ELEMENT NUMBER

6. AUTHOR(S)
Ming C. Wu and Connie Chang-Hasnain

5d. PROJECT NUMBER

5e. TASK NUMBER

5f. WORK UNIT NUMBER

7. PERFORMING ORGANIZATION NAME(S) AND ADDRESS(ES)
University of California, Berkeley
2150 Shattuck Ave. Suit 300
Berkeley, CA 94704-5940

8. PERFORMING ORGANIZATION REPORT NUMBER

9. SPONSORING/MONITORING AGENCY NAME(S) AND ADDRESS(ES)
US ARMY RDECOM ACQ CTR - W911NF
4300 S. Miami Blvd
Durham NC 27703

10. SPONSOR/MONITOR'S ACRONYM(S)

11. SPONSOR/MONITOR'S REPORT NUMBER(S)

12. DISTRIBUTION/AVAILABILITY STATEMENT
Approved for public releases, distribution unlimited

13. SUPPLEMENTARY NOTES

14. ABSTRACT

Directly modulated semiconductor lasers are the most compact optoelectronic sources for analog (microwave) as well as digital photonic systems. The bandwidth of semiconductor lasers has been limited by relaxation oscillation frequency to < 40 GHz. By using strong optical injection locking, we report resonance frequency enhancement in excess of 100 GHz in semiconductor lasers. We demonstrate this enhancement experimentally in both distributed feedback (DFB) lasers and vertical-cavity surface-emitting lasers (VCSELs), showing the broad applicability of the technique and that the coupling Q (optical quality factor) is the figure-of-merit for resonance frequency enhancement. We have also identified the key factors that cause low-frequency roll-off in injection-locked lasers. By increasing the slave laser's DC current bias, we have achieved a record intrinsic 3-dB bandwidth of 80 GHz in VCSELs.

15. SUBJECT TERMS
RF photonics, microwave photonics, high speed modulation, optical injection locking, semiconductor laser

16. SECURITY CLASSIFICATION OF:			17. LIMITATION OF ABSTRACT	18. NUMBER OF PAGES	19a. NAME OF RESPONSIBLE PERSON
a. REPORT	b. ABSTRACT	c. THIS PAGE			USARME
U	U	U	UU	13	19b. TELEPHONE NUMBER *(Include area code)*

FINAL PROGRESS REPORT (FPR)

Grant Number:
W911NF-07-1-0468

Project Title:
High Speed Laser with > 100 GHz Resonance Frequency

Principal Investigator:

Ming C. Wu
University of California, Berkeley

Table of Contents:

I. Statement of the problem studied

To support the growing need for larger transmission speeds in optical communications, much research has been devoted to increasing the direct modulation bandwidth of semiconductor lasers. In a typical laser, the relaxation oscillation (resonance) frequency is a figure-of-merit that is a necessary but not sufficient condition for determining its maximum direct modulation bandwidth. The resonance frequency of directly modulated lasers has been demonstrated up to ~30 GHz. Practical limitations, including laser heating and gain compression, limit the maximum resonance frequency. Furthermore, increased damping at higher resonance frequencies limit the maximum bandwidth to 30-40 GHz.

Previously, we have shown that strong optical injection locking can significantly enhance the resonance frequency of semiconductor lasers. In past works, however, low-frequency roll-off has limited the bandwidth of the enhanced-resonance lasers to well-below the resonance frequency, reducing the high-frequency uses to narrow-band applications, such as opto-electronic oscillators. Recently, however, by optimizing the detuning frequency and injection ratio, we have shown enhanced bandwidths of up to 44 GHz, This already surpasses the record bandwidths achieved by any semiconductor laser.

II. Summary of the most important results

In this research, we significantly expand the high-frequency capabilities of optical injection-locked lasers. First, we develop a theoretical model for the resonance frequency and bandwidth enhancement. The model shows that the maximum resonance frequency is inversely proportional to the coupling Q-factor, and also increases as the injection power and optical frequency increase. Additionally, we show that lasers with very different cavity dimensions but similar Q-factors will demonstrate similar resonance frequency enhancement. These conclusions are verified experimentally. We use these design rules to maximize the resonance frequency. We have achieved resonance frequencies >100 GHz in both optical injection-locked (OIL) 1550-nm distributed-feedback (DFB) and vertical-cavity surface-emitting lasers (VCSELs). In addition, we use the model to describe the source of the low-frequency roll-off and delineating the key laser parameters that can be used to reduce the roll-off and increase the laser bandwidth. We show that by increasing the DC

bias current of the slave, the modulation bandwidth can be enhanced significantly. By optimizing the slave laser bias, we demonstrate intrinsic 3-dB bandwidths up to 80 GHz. These results have been published in journals [1]–[10].

A. Theory

We have developed a small-signal, linearized theoretical model that describes the injection-locked laser system. Using this model, we approximated the resonance frequency of an injection-locked laser as

$$\omega_R^2 = \omega_{R0}^2 + \Delta\omega_R^2 \quad (1)$$

where ω_R and ω_{R0} are the injection-locked and free-running resonance frequency, respectively. $\Delta\omega_R$ is the resonance frequency enhancement term:

$$\Delta\omega_R = \left|\kappa\sqrt{R_{inj}}\sin(-\phi_0)\right| \quad (2)$$

where κ (= $1/\tau_{rt}$) is the coupling coefficient; τ_{rt} is the cavity round-trip time; R_{inj} is the internal injection ratio, defined as the ratio of optical powers of the master and free-running slave laser inside the slave laser cavity; and ϕ_0 is the phase difference between slave and master fields. For low injection ratios, the enhancement is small and the resonance frequency of the injection-locked laser is dominated by the free-running laser frequency. With increasing injection power, the resonance frequency can increase dramatically. Similarly, as the detuning frequency moves to the positive edge of the locking range, ϕ_0 approaches $-\pi/2$, thereby increasing ω_R. Finally, κ is inversely proportional to the cavity round-trip time. Therefore, with a shorter cavity, we can see an additional increase in resonance frequency.

The slave laser can be of any type; here we take a distributed feedback (DFB) laser and a vertical-cavity surface-emitting laser (VCSEL) as two examples with very different cavity designs. The VCSEL's effective cavity length is much shorter, resulting in a higher κ for the VCSEL, though the high mirror reflectivity of the VCSEL reduces the amount of light transmitted into the cavity and, hence, reduces the internal injection ratio.

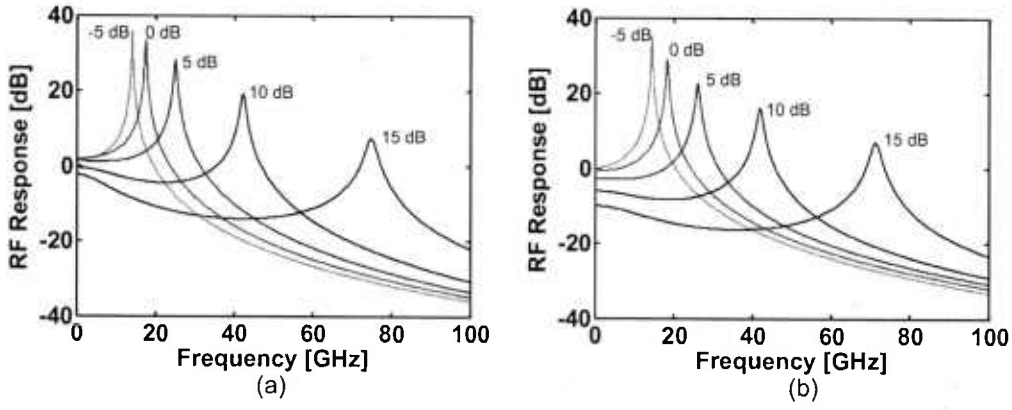

Fig. 1. Frequency response comparison between (a) DFB and (b) VCSEL, both with Q_c = 6800. Each response curve shows the maximum resonance frequency for a given injection ratio, labelled on the curve. The maximum resonance frequency of each laser is the same for any given injection ratio.

Quantitatively, the maximum resonance frequency enhancement, $\Delta\omega_{R,max}$, can be written as

$$\Delta\omega_{R,max} = \frac{\omega_0}{2Q_c}\sqrt{R_{ext}} \tag{3}$$

where ω_0 is the laser angular frequency; Q_c is the coupling quality factor of the slave laser cavity (from output mirrors); and R_{ext} is the external injection ratio, defined as the ratio of optical powers of the incident master and free-running slave laser just outside of the slave laser facet. As discussed in, the Q-factor of a typical DFB and VCSEL are roughly equivalent: on the order of several 1000's. Therefore, we would expect the maximum resonance frequencies to be approximately the same for the two laser systems. In Section 3, we show this experimentally. In fact, any laser of similar Q_c should exhibit similar maximum resonance frequencies. Fig. 1 shows a comparison of the frequency response of a DFB and VCSEL, both with Q_c = 6800. This was accomplished by modeling the DFB length and effective mirror reflectivity to be 500 μm and 0.3, respectively and the VCSEL length and mirror reflectivity to be 2 μm and 0.995, respectively. The small-signal model was based on the standard rate equations. The responses are for different injection ratios, and the maximum resonance frequency for each injection ratio is shown. The comparison shows that both lasers exhibit the same maximum resonance frequencies at any given injection ratio. Note that the DC response is normalized to the free-running laser DC response. At the extreme positive detuning edge (highest resonance frequency), the DC response can drop. This is not necessarily the case for detunings away from the edge. While the DC response may decrease slightly with increasing resonance frequency, the magnitude can often be equal or larger than the free-running DC response, as shown in experiment and theory. Thus, the injection-locked system can give DC gain as well as enhanced resonance frequency.

Although the resonance frequency of an injection-locked laser has been shown to be enhanced significantly higher than that achievable by conventional lasers, the modulation response typically drops sharply, rolling off close to DC before being enhanced by the resonance frequency. This produces poor response between DC and resonance, in contrast to conventional lasers, whose response is typically flat or rising from DC to resonance. This "sagging" response is evident in all strong injection locking experiments showing significant resonance enhancement, and has limited the 3-dB bandwidths of these prior works. The roll-off is due to an additional real pole that appears in directly-modulated OIL systems, and is distinct from the RC parasitics. The real pole acts like a low-pass filter whose cut-off frequency, ω_P, changes dynamically with the injection locking conditions, and has been observed to be as low as a few GHz. In this section, we explain this phenomenon physically and quantitatively provide design rules to mitigate the low-frequency roll-off, in order to improve the modulation bandwidth.

We can develop some physical intuition to the roll-off through the small-signal model. In a non-injection-locked (free-running) laser, the resonance frequency is induced by the coupling of carriers and photons. Using direct modulation, carriers are directly injected into this coupling, and we exhibit a classic 2-complex-pole behavior. In an injection-locked laser, however, the enhanced resonance frequency is induced by the coupling between the photon amplitude and phase, due to the beating between master and slave cavity mode frequencies. Hence, the directly-modulated carriers are no longer injected directly into the resonance frequency energy reservoirs. The transfer of energy from the carriers to the resonance is then dominated by the carrier relaxation rate, enhanced by stimulated emission.

Quantitatively, we can approximate the cut-off frequency of the low-frequency roll-off as

$$\omega_P \approx \left[1 + \frac{2\alpha Q_c}{\sqrt{R_{ext} Q_{tot}}} \sin(-\varphi_0)\right] g S_0 \qquad (4)$$

where α is the linewidth enhancement parameter, Q_{tot} is the total cavity-Q (from mirror and internal loss), g is the differential gain, and S_0 is the photon number in the slave cavity. To maximize bandwidth we must increase the low-pass pole frequency. As the detuning increases, despite the fact that the sine term approaches unity, the resonance frequency goes up, forcing ω_P to smaller values. In order to maximize ω_P, there are several design parameters to utilize: 1) use lasers with higher α, 2) increase the injection ratio to increase S_0, 3) increase the differential gain, and 5) increase the photon number. Of course, there are design trade-offs or fundamental limits with changing many of these parameters. The most straightforward of these methods is to increase the photon number, specifically by increasing the slave laser current bias. By increasing the photon number (via bias current), we can increase the low-pass pole frequency until it no longer dominates the frequency response below resonance. Effectively, we are increasing the carrier decay rate by enhancing the stimulated emission in the cavity. Fig. 2(a) shows the dependency of frequency response on the bias current. Here, we have fixed both injection ratio and resonance frequency while increasing bias current. For a current of $4\times J_{th}$, we can increase the bandwidth from a few GHz to > 60 GHz. Fig. 2(b) shows a near-linear relationship between pole frequency and photon number (which is proportional to J-J_{th}). It is important to note that the pole need not be enhanced as high as the resonance frequency to achieve large 3-dB bandwidths. As we see in Fig. 2(b) for $4\times J_{th}$, only a modest enhancement to 20 GHz is necessary to achieve 60 GHz bandwidths. Additional increases in the bias yields marginal improvements to the bandwidth. The corresponding free-running, 3-dB bandwidths are shown as well. We see that the free-running laser is only capable of ~20 GHz bandwidth.

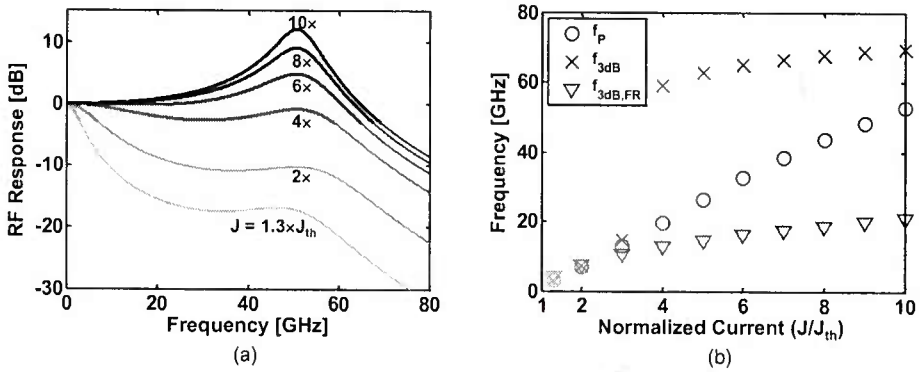

Fig. 2. (a) Dependence of the frequency response on bias current. Thick, overlain lines show the 3-dB frequency range. (b) Dependence of the low-pass pole frequency, f_P, to current, along with corresponding 3-dB frequencies, f_{3dB}. The 3-dB bandwidth of the free-running laser is also shown ($f_{3dB,FR}$).

B. Experimental results

Here, we record the results from our experimental investigation of the theoretical concepts presented in the previous section. First, we demonstrate the dependency of Q_c on the maximum resonance frequency, while simultaneously demonstrating >100 GHz resonance frequencies in DFB lasers and VCSELs. Then we demonstrate the concept of bandwidth enhancement by increasing current bias, reporting up to 80 GHz intrinsic bandwidths.

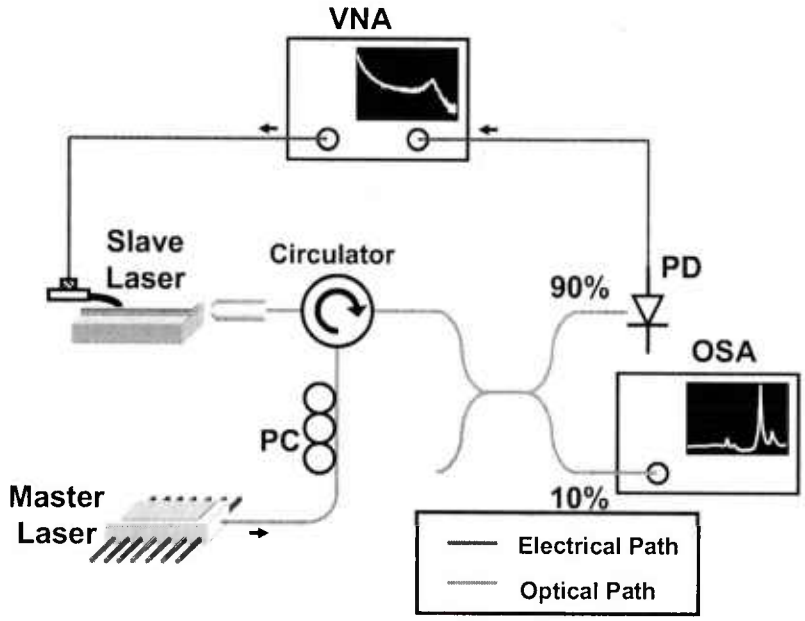

Fig. 3. Optical injection locking experimental setup. VNA: vector network analyzer, PD: photodetector, OSA: optical spectrum analyzer, PC: polarization controller.

The experimental setup is shown in Fig. 3. We compared the injection locking performance of two slave lasers (SL): a 1550 nm DFB laser and a 1550 nm VCSEL. For the DFB, injection light was coupled using an anti-reflection-coated lensed optical head with ~50% coupling efficiency. For the VCSEL, we used a lensed fiber with ~70% coupling efficiency. The master laser is a commercial, high-power (18-dBm) DFB laser. Frequency detuning of the master laser was performed by temperature tuning. A variable optical attenuator was used to change the power of the master laser. A polarization controller was used in the experiments to match the polarizations of the master and slave lasers. A circulator was used to allow simultaneous injection and measurement to the slave laser, while reducing feedback to the master laser. The slave laser is directly modulated by a RF signal using a 1-mm coaxial microwave signal-ground probe, sourced by a 110-GHz vector network analyzer (VNA) (Agilent N5250A). A 90/10 coupler was used to measure the light simultaneously on the VNA and a 10-pm resolution bandwidth optical spectrum analyzer (OSA). The light is converted to an electrical signal via a 100-Gbps photodetector (PD) (Fraunhofer C05-W31). The frequency response was normalized for cable, VNA, and PD loss, but probe loss could not be de-embedded due to non-planar probe contacts.

C. Injection Locking of DFB Lasers

The DFB used was a 500-μm long, 1.55 μm InGaAsP DFB laser with a threshold of 8 mA at 20°C. The DFB is biased at 31.7 mA ($1.3\times I_{th}$) at 60°C (to match the wavelength range of the ML); its optical power is 1 dBm. The frequency response of the free-running DFB laser is shown by the black curve in Fig. 4(a), having a free-running relaxation oscillation frequency of 3 GHz. Under strong optical injection, the frequency response exhibits significant enhancement. We inject the DFB with a master laser output power of 18 dBm. With the 50% coupling efficiency of the optical head and about 1 dB of insertion loss in other components, this results in an injection ratio of ~14 dB. The colored curves of Fig. 4(a) show the frequency response for the injection-locked DFB; holding the injection ratio constant, the detuning frequency was varied from -47 to +67 GHz, with a step size of ~12.7 GHz. This resulted in a resonance frequency increase from 45 to 107 GHz, respectively. These results are limited only by the 110-GHz source and detection equipment we used, and is not limited by the injection-locked laser itself. For example, we can increase the resonance frequency further by increasing the detuning and/or injection ratio. The migration of the resonance to higher frequencies and the decrease in damping is clearly shown as the detuning frequency is increased. The increased noise at 67 GHz is due to a dip in the VNA response as it transitions its source to external mixers, resulting in an increase in the noise floor. The corresponding optical spectra (without modulation) for each detuning frequency is shown in Fig. 4(b). The main locked mode can be seen as it detunes from long to shorter wavelengths. The cavity mode can be easily identified on the long wavelength side of the main locked mode. As we increase the detuning frequency, we can see the locked mode pull away from the cavity mode. The frequency difference between locked and cavity mode equals the resonance frequency shown in the frequency response curves. Additionally, the un-modulated cavity mode power increases with detuning, resulting in the reduction of resonance damping, also evident in the frequency response curves. The side-mode suppression ratio (SMSR) remains > 30 dB for all detuning values.

The 107-GHz resonance frequency case represents a 34 times increase in the resonance frequency over the 3-GHz of the free-running laser. The DC levels of both free-running and 107-GHz case are equal. The RF response at the resonance peak (107 GHz) is 12 dB below the DC level. This can be raised higher than the DC level by mitigating the package parasitics of the slave laser or using impendence matching. In Fig. 4(c), we plot the frequency response while holding the SMSR constant at 30 dB and varying the injection ratio from 6 to 14 dB. We again see that the resonance frequency increases, this time with rising injection ratio. The corresponding optical spectrum is shown in Fig. 4(d). The sensitivity setting was decreased, resulting in a higher noise floor than Fig. 4(b). Fig. 4(e) shows the resonance frequency enhancement over the entire locking map by extracting the resonance frequency over the parameter space. The contour plot shows that increasing either the injection power or the master laser frequency will result in increased resonance frequency.

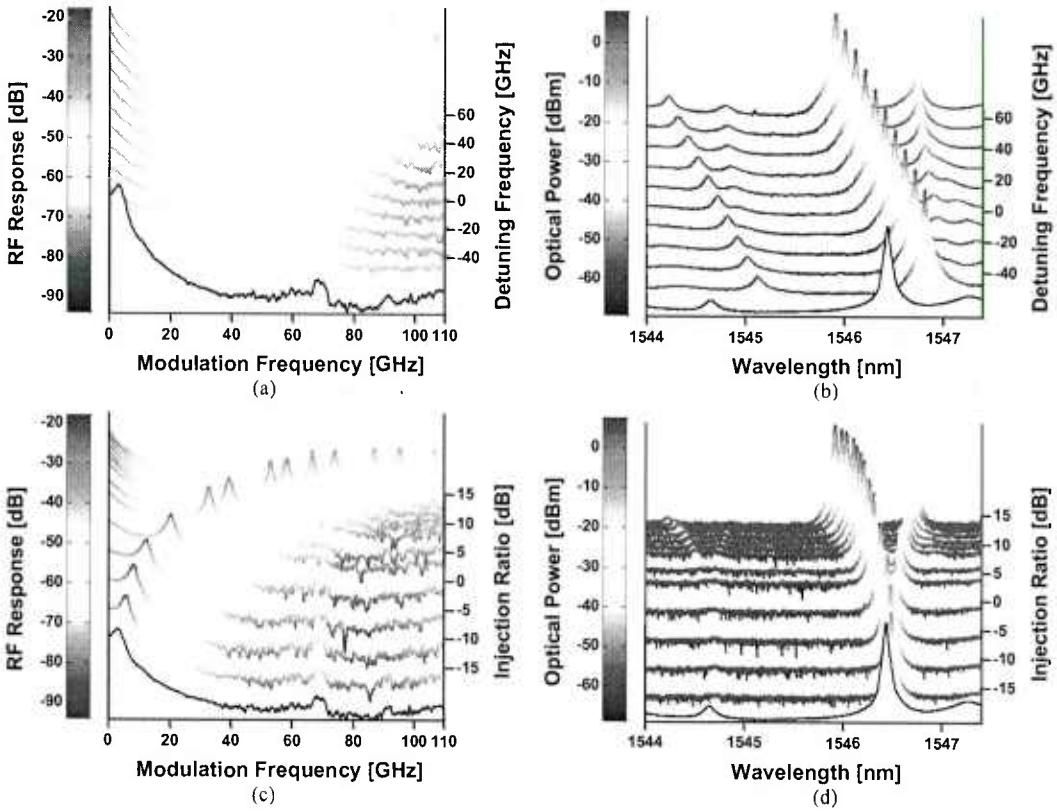

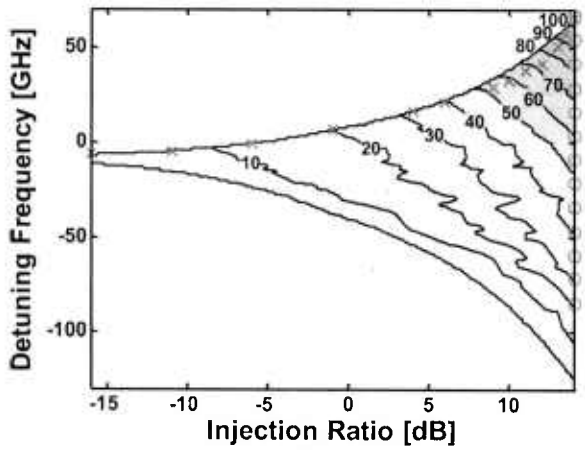

(e)

Fig. 4. Evolution of injection-locked laser across locking range: (a) DFB frequency response and (b) corresponding optical spectra for +14 dB injection ratio. The detuning frequencies are varied from -47 to +67 GHz, in 12.7 GHz increments. The solid black lines represent the free-running case. The curves are offset for clarity. (c) DFB frequency response for different injection ratios (-16, -11, -6, -1, 4, 6, 9, 10, 11, 12, 13, 13.5 and 14 dB) and (d) corresponding optical spectra. (e) DFB resonance frequency as a function of detuning frequency and injection ratio, contour plot. Red O- and green X-marks are the bias points from (a) and (c), respectively. Frequency response curves in (a) and (c) are smoothed 0.5% for clarity.

D. Injection Locking of VCSELs

For the VCSEL experiments, we used a 1.55 μm VCSEL with a threshold of 0.6 mA. Due to the increased sensitivity to polarization effects in the VCSEL case, polarization-maintaining components were used in lieu of a polarization controller. We also used a 99/1 optical coupler to split the modulated light between the photodetector and OSA. The other experimental details are the same as in the DFB case. Fig. 5(a) shows the frequency response when biased at 1.8 mA ($3\times I_{th}$, 0.43 mW output power) with and without injection locking. The free-running slave laser (shown in black) has a resonance frequency of 5 GHz. When locked with an injection ratio of +13.6 dB, the detuning frequencies of the curves (shown in color) were varied from +88 GHz to +102 GHz. This resulted in resonance frequencies from 92 to 104 GHz. Again, these results are limited only by the source/detection equipment, not by the injection-locked laser itself. As shown, the maximum resonance frequency is >100 GHz, which is approximately the same as the DFB results in Section 3.2. This is a >20 times increase in the free-running resonance frequency. The corresponding optical spectrum is shown in Fig. 5(b).

Since the maximum resonance frequency of both the VCSEL and DFB are similar (~104-7 GHz), we can equate Eq. (3) for both lasers. We have experimentally estimated that the Q_c

of both lasers are approximately equal ($Q_c \approx$ 5-6000 for the VCSEL, $Q_c \approx$ 5570 for the DFB). Also, since the injection ratios and wavelengths are approximately equal (R_{ext} = 13.6 dB for the VCSEL, R_{ext} = 13 dB for the DFB, both at $\lambda_0 \approx$ 1.55 μm), this verifies Eq. (3). This is an important note, given the extremely different laser designs, cavity lengths, mirror reflectivities, and geometries. Hence, this shows that the coupling Q-factor is a more accurate and fundamental metric for determining resonance frequency enhancement.

Although there is no theoretical limit to the resonance frequency enhancement, the practical limit occurs when the detuned master laser encounters the next-order laser modes (i.e. Fabry-Perot modes). Our current DFB slave laser benefits from the wide (~1.8 nm) forbidden zone of the DFB structure, while the VCSEL's mode spacing (aside from polarization modes) is even larger due to its extremely short cavity. Hence, the cavity must be engineered to ensure the spacing of these modes is far apart to support the desired resonance frequencies.

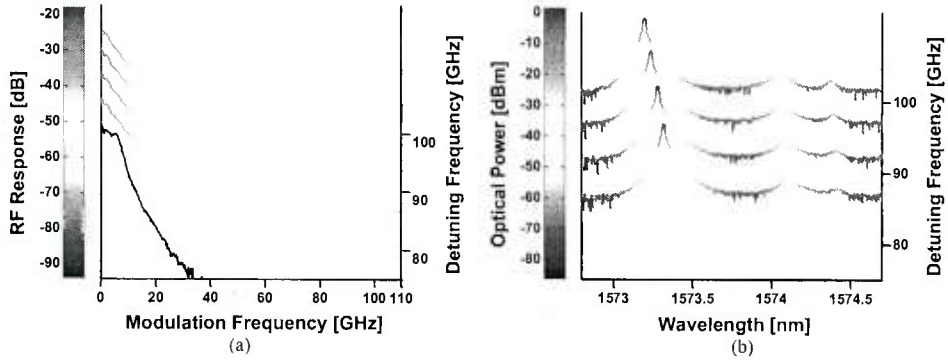

Fig. 5. Evolution of injection-locked VCSEL for different detuning frequencies: (a) frequency response (smoothed 0.5% for clarity) and (b) corresponding optical spectra for +13.6 dB injection ratio. The detuning frequencies are 88, 93, 98, and 102 GHz. The solid black line represents the free-running case. The curves are offset for clarity.

The common feature in the frequency response curves in Fig. 4(a) and 5(a) is the drop in response starting near DC that severely limits the 3-dB bandwidth of the frequency response. The response drops well below 3-dB close to DC and well before the resonance frequency is reached. This is in contrast to a free-running laser, whose 3-dB bandwidth is typically larger than the resonance frequency, since the classic laser system does not exhibit this low-frequency low-pass pole.

We have discussed the various design rules that can be used to increase the low-pass pole frequency in Section 2.2. Here, we focus on enhancing the pole frequency by increasing the photon density (via the slave laser bias current). Our experimental results are shown in Fig. 6(a), which shows the effects of bias current on the frequency response. We increase the bias current while keeping the injection ratio (~12-13 dB) and resonance frequency (~68 GHz) constant. The injection ratio was chosen such that the resonance frequency would be detuned well away from the positive locking edge, resulting in larger damping, less non-

linearity, higher DC gain, and a flatter response curve. The two experimental VCSEL frequency response curves (dotted) for 1.3× and 5×I_{th} are plotted after de-embedding the RC pole, which we found to be 16 GHz. The pole was determined to be consistent by a fit over a wide range of resonance frequencies. The free-running output powers were -11 and -0.86 dBm, respectively. When biased at 1.3×I_{th}, the low-pass pole limits the 3-dB bandwidth to ~1 GHz. However, with a bias of 5×I_{th}, the 3-dB bandwidth extends beyond the resonance frequency, demonstrating an intrinsic 3-dB bandwidth of 80 GHz. Theoretical curves (solid), based on a small-signal analysis of the classic rate equations, were calculated. The VCSEL parameters were: V = 6×10^{-13} cm^{-3}; g = 4.14×10^{5} s^{-1}; N_{th} = 2.4×10^{6}; α = 12; J_{th} = 2.4×10^{15} s^{-1}; γ_n = 1 ns^{-1}; γ_p = 700 ns^{-1}; L = 1.12 μm; r = 0.99. The injection ratio was kept at ~ 4 dB while the detuning was tuned to achieve a resonance frequency of 68 GHz. The discrepancy in the theoretical and experimental injection ratios may be due to the inaccuracies of the estimation of the coupling efficiencies. Nevertheless, the theory shows excellent agreement with the experiment. The linearization of the injection locking rate equations resulted in a frequency response composing of 2 complex poles (producing the resonance frequency and damping) and 1 real pole (producing the low-pass roll-off). The theory curves predict bandwidths of 1.4 and 80 GHz for the bias cases of 1.3× and 5×I_{th}. An additional theoretical frequency response curve at 9×I_{th} is shown, showing the clear trend of bandwidth enhancement with increasing slave laser bias current. Fig. 6(b) show the extracted pole frequencies from the experimental curves. The figure also shows that we only need a pole enhancement up to ~20 GHz (by biasing to 5×I_{th}) to achieve 80-GHz 3-dB bandwidth. Hence, with a higher power master laser, we expect to push the bandwidth to higher frequencies. We also expect to overcome the electrical parasitics with superior packaging and/or laser design. Finally, the DC response for the 1.3× and 5×I_{th} bias levels are +3 and -1 dB, respectively, relative to the free-running DC response, showing virtually no penalty to the overall response.

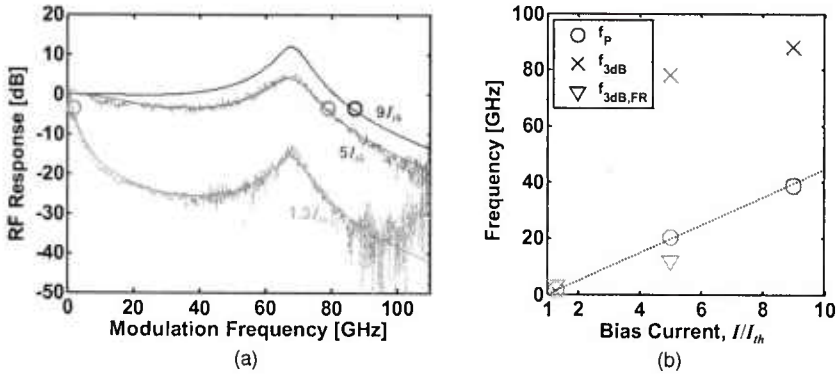

Fig. 6. (a) Experimental and theoretical frequency responses of optical injection-locked VCSEL at different DC bias currents. Experimental VCSEL curves (dotted) are shown for I = 1.3× and 5×I_{th}. Theoretical curves (solid) are shown for I = 1.3×, 5×, and 9×I_{th}. 3-dB frequencies of 1.4 and 80 GHz for the experimental curves, respectively, are shown in circles. (b) Extracted low-pass pole values (f_P) for the three

bias points, with corresponding 3-dB frequencies (f_{3dB}). Experimental free-running 3-dB frequencies also marked ($f_{3dB,FR}$).

E. Summary

In this work, we have used optical injection locking to enhance the resonance frequency beyond 100 GHz and demonstrated intrinsic 3-dB bandwidths up to 80 GHz. While these are, to the authors' knowledge, the highest recorded resonance frequency and intrinsic bandwidth in continuous-wave, room-temperature semiconductor lasers, we expect to exceed these records in the near future, as we have not reached the fundamental limits of the frequency enhancement. We have also determined that the coupling Q-factor is the dominant metric for determining maximum resonance frequency enhancement. Since optical injection locking is a universal technique, applicable to any laser, using Q as a universal figure of merit is very useful for comparing very different lasers, such as the DFB laser and VCSEL used in these experiments. The design trade-off to be made is the desire for a low Q for a large resonance frequency, but a high Q for low threshold current. A comparison between semiconductor, fiber, or solid-state lasers would be of great interest. Finally, the extremely high bandwidth, dynamically tunable resonance frequency, and universal applicability make optical injection locking a very flexible and powerful technique.

III. Publications

[1] E. K. Lau, H.-K. Sung, and M. C. Wu, "Scaling of resonance frequency for strong injection-locked lasers," *Opt. Lett.*, vol. 32, no. 23, pp. 3373–3375, Dec. 2007.

[2] H.-K. Sung, E. K. Lau, and M. C. Wu, "Optical Properties and Modulation Characteristics of Ultra-Strong Injection-Locked Distributed Feedback Lasers," *IEEE J. Sel. Top. Quantum Electron.*, vol. 13, no. 5, pp. 1215–1221, 2007.

[3] H.-K. Sung, E. K. Lau, and M. C. Wu, "Optical Single Sideband Modulation Using Strong Optical Injection-Locked Semiconductor Lasers," *IEEE Photonics Technol. Lett.*, vol. 19, no. 13, pp. 1005–1007, 2007.

[4] X. Zhao, D. Parekh, E. K. Lau, H. K. Sung, M. C. Wu, W. Hofmann, M. C. Amann, and C. J. Chang-Hasnain, "Novel cascaded injection-locked 1.55-μm VCSELs with 66 GHz modulation bandwidth," *Opt. Express*, vol. 15, no. 22, pp. 14810–14816, 2007.

[5] E. K. Lau, H.-K. Sung, and M. C. Wu, "Frequency Response Enhancement of Optical Injection-Locked Lasers," *Quantum Electron. IEEE J. Of*, vol. 44, no. 1, pp. 90–99, 2008.

[6] E. K. Lau, L. J. Wong, X. Zhao, Y.-K. Chen, C. J. Chang-Hasnain, and M. C. Wu, "Bandwidth Enhancement by Master Modulation of Optical Injection-Locked Lasers," *J Light. Technol*, vol. 26, no. 15, pp. 2584–2593, 2008.

[7] E. K. Lau, X. Zhao, H.-K. Sung, D. Parekh, C. Chang-Hasnain, and M. C. Wu, "Strong optical injection-locked semiconductor lasers demonstrating > 100-GHz resonance frequencies and 80-GHz intrinsic bandwidths," *Opt. Express*, vol. 16, no. 9, pp. 6609–6618, Apr. 2008.

[8] E. K. Lau, A. Lakhani, R. S. Tucker, and M. C. Wu, "Enhanced modulation bandwidth of nanocavity light emitting devices," *Opt. Express*, vol. 17, no. 10, pp. 7790–7799, 2009.

[9] E. K. Lau, L. J. Wong, and M. C. Wu, "Enhanced Modulation Characteristics of Optical Injection-Locked Lasers: A Tutorial," *Sel. Top. Quantum Electron. IEEE J. Of*, vol. 15, no. 3, pp. 618–633, 2009.

[10] H.-K. Sung, X. Zhao, E. K. Lau, D. Parekh, C. J. Chang-Hasnain, and M. C. Wu, "Optoelectronic Oscillators Using Direct-Modulated Semiconductor Lasers Under Strong Optical Injection," *Sel. Top. Quantum Electron. IEEE J. Of*, vol. 15, no. 3, pp. 572–577, 2009.